Radiative pion capture and pion photoproduction in a chiral bag model

A. N. Kamal
Department of Physics and Theoretical Physics Institute, University of Alberta, Edmonton, Canada T6G 2J1

M. Araki
Institut für Kernphysik, Universität Mainz, 6500 Mainz 1, Federal Republic of Germany
(Received 22 January 1988)

Radiative pion capture on nucleons is studied in a chiral bag model at pion laboratory momenta in the range $q_L \sim 300$–500 MeV. We calculate $d\sigma/d\Omega$ and L-R asymmetry. Through detailed balance and time reversal invariance we also calculate $d\sigma/d\Omega$ and $P(\theta)$ (nucleon recoil polarization) for pion photoproduction at equivalent photon laboratory momenta. A detailed comparison is made with the data.

I. INTRODUCTION

After the inception of the MIT bag model,[1] chiral symmetry was first built into the model by coupling the pion field to the quarks through a pseudoscalar (PS) coupling at the surface of the bag. In this model[2]—the cloudy bag model—the pion field was thereby excluded from the interior of the bag. This picture had a good deal of success in describing the axial vector coupling constant, g_A, and $I(\text{isospin})=\frac{3}{2}$, $J=\frac{3}{2}$, P-wave Δ resonance.

However, it is well known that at the nucleon level the pseudoscalar theory[3] has difficulty in explaining pion-nucleon S-wave scattering lengths in $I=\frac{1}{2}$ and $\frac{3}{2}$ states, a_1 and a_3, in particular their individual small sizes and their ratio $a_1/a_3 \simeq -2$. Not that the PS theory is fundamentally flawed, but that the Born terms produce very large S-wave scattering lengths of the same sign. The contribution of higher resonances and the continuum has to be included to produce agreement with low-energy pion-nucleon scattering data.

On the other hand, a pseudovector (PV) coupling of the pions with the nucleons has the advantage that at the Born level it reproduces the low-energy data and, theoretically, the results of low-energy current algebra theorems.[4] In this sense the PV theory has the advantage of simplicity and wieldiness over the PS theory *at low energies.*

In order to describe low-energy S-wave pion-nucleon scattering data, the cloudy bag model was modified[5] by transforming the quark field in a manner that the effective theory became a PV theory, nonlinear in the pion field which became nonzero inside the bag. In this manner an agreement was secured[5] with S-wave πN scattering data.

A chiral bag model was proposed by Kälberman and Eisenberg[6] who devised a nonlinear σ model at the quark level. Such a nonlinear chiral bag introduces a PV coupling throughout the bag volume and naturally reproduces the correct S-wave low-energy πN scattering data. The models of Refs. 5 and 6 differ in cubic and higher-order terms in the pion field.

In an earlier publication[7] we had investigated pion photoproduction in chiral bag models. In the present paper we address the problem of radiative pion capture in the Kälberman-Eisenberg[6] chiral bag model. Time-reversal invariance allows us to infer the differential cross section and the recoil nucleon polarization in the pion photoproduction process at an equivalent photon energy. We believe that our present calculation is more reliable, especially at small angles since both the cross section and the polarization are calculated from the total amplitudes. In Ref. 7 these quantities were computed from low-order multipoles. The emphasis in Ref. 7 was on multipole analysis.

The layout of this paper is as follows. We present a calculation of radiative pion capture [$d\sigma/d\Omega$ and the left-right (L-R) asymmetry] at the nucleon level in Sec. II. We employ a PV coupling of the pion with nucleons. We also include the contribution of $\Delta(1232)$. In Sec. III we do the same calculation at the bag level and show what replacements lead us to the bag description. Finally in Sec. IV we present our results with a discussion.

II. A CALCULATION OF RADIATIVE PION CAPTURE AT THE NUCLEON LEVEL

We start with a calculation of radiative π capture at the nucleon level. We use a PV coupling of the pion with the nucleons and evaluate the amplitude at the tree level where the contribution from the nucleon, the Δ resonance and the pion poles and the seagull term are retained. Our model is defined through the following Langrangian densities,[8]

$$\mathcal{L}=\mathcal{L}_{\pi NN}+\mathcal{L}_{\gamma NN}+\mathcal{L}_{\gamma\pi\pi}+\mathcal{L}_{\gamma\pi NN}+\mathcal{L}_{\pi N\Delta}+\mathcal{L}_{\gamma N\Delta}\ , \tag{1}$$

where (we use the Bjorken and Drell[9] convention)

$$\mathcal{L}_{\pi NN}=\frac{f}{m_\pi}\bar{\psi}\gamma_5\gamma_\mu\tau\cdot\partial^\mu\phi\psi \tag{2}$$

with $f^2/4\pi=0.08$ and m_π the pion mass, and

$$\mathcal{L}_{\gamma NN}=-e\bar{\psi}\left[\frac{1+\tau_3}{2}\right]A\psi-\frac{e}{4m}\bar{\psi}\sigma_{\mu\nu}(\kappa^S+\tau_3\kappa^V)\psi F^{\mu\nu}\ , \tag{3}$$

where m is the nucleon mass and the scalar and the vector anomalous moments of the nucleons are

$$\kappa^S=\tfrac{1}{2}(\kappa_p+\kappa_n)=-0.06\ ,$$
$$\kappa^V=\tfrac{1}{2}(\kappa_p+\kappa_n)=1.85\ . \tag{4}$$

Electromagnetic interaction of the pion and the seagull interaction are

$$\mathcal{L}_{\gamma\pi\pi}=-e\epsilon^{ab3}\partial_\mu\phi^a\phi^b A^\mu\ ,$$
$$\mathcal{L}_{\gamma\pi NN}=-\frac{ef}{m_\pi}\epsilon^{ab3}\bar{\psi}\gamma_5\tau^a \mathcal{A}\psi\phi^b\ . \tag{5}$$

The interactions involving Δ (1236) are assumed to be[7,8]

$$\mathcal{L}_{\pi N\Delta}=g^*\bar{\psi}^\mu_\Delta \mathbf{T}\cdot\partial_\mu\boldsymbol{\phi}\psi\ ,$$
$$\mathcal{L}_{\gamma N\Delta}=iec\bar{\psi}^\mu_\Delta T_3\gamma^\nu\gamma_5\psi F_{\mu\nu}\ , \tag{6}$$

where we use[8] $g^*=1.9m_\pi^{-1}$ and $c=0.32/m_\pi$. ψ^μ_Δ represents the Δ spinor and T_i are the 4×2 isospin matrices with the following representation:[10]

$$T_1=\frac{1}{\sqrt{2}}\begin{bmatrix}1&0\\0&1/\sqrt{3}\\-1/\sqrt{3}&0\\0&-1\end{bmatrix},\quad T_2=-\frac{1}{\sqrt{2}}\begin{bmatrix}i&0\\0&i/\sqrt{3}\\i/\sqrt{3}&0\\0&i\end{bmatrix},\quad T_3=-\sqrt{\tfrac{2}{3}}\begin{bmatrix}0&0\\1&0\\0&1\\0&0\end{bmatrix}. \tag{7}$$

With $\bar{\psi}_\Delta=(\bar{\Delta}^{++},\bar{\Delta}^{+},\bar{\Delta}^{0},\bar{\Delta}^{-})$ these isospin matrices generate the following isospinors:

$$\bar{\psi}_\Delta T_1=\frac{1}{\sqrt{2}}(\bar{\Delta}^{++}-\bar{\Delta}^{0}/\sqrt{3},\bar{\Delta}^{+}/\sqrt{3}-\bar{\Delta}^{-})\ ,$$
$$\bar{\psi}_\Delta T_2=-\frac{i}{\sqrt{2}}(\bar{\Delta}^{++}+\bar{\Delta}^{0}/\sqrt{3},\bar{\Delta}^{+}/\sqrt{3}+\bar{\Delta}^{+})\ , \tag{8}$$
$$\bar{\psi}_\Delta T_3=-\sqrt{\tfrac{2}{3}}(\bar{\Delta}^{+},\bar{\Delta}^{0})\ .$$

T_i satisfy the following relations which are useful in projecting out the isospin amplitudes:

$$T^\dagger_\beta T_\alpha=\delta_{\beta\alpha}-\tfrac{1}{3}\tau_\beta\tau_\alpha \tag{9}$$

from which we get

$$T^\dagger_3 T_\alpha=\tfrac{2}{3}\delta_{\alpha\beta}+\tfrac{1}{6}[\tau_\alpha,\tau_3]\ ,$$
$$T^\dagger_\alpha T_3=\tfrac{2}{3}\delta_{\alpha\beta}-\tfrac{1}{6}[\tau_\alpha,\tau_3]\ . \tag{10}$$

The Δ propagator in the zero width limit is given by

$$i\left[g_{\mu\nu}-\frac{1}{3}\gamma_\mu\gamma_\nu-\frac{1}{3m_\Delta}(\gamma_\mu P_\nu-P_\mu\gamma_\nu)-\frac{2}{3}\frac{P_\mu P_\nu}{m^2_\Delta}\right]\frac{1}{(\not{p}-m_\Delta)}\ . \tag{11}$$

In our calculation we have used a finite width of 120 MeV by modifying the denominator in (11).

With the Lagrangian of (1)–(6) we compute the tree level amplitude for radiative π capture on a nucleon

$$\pi^\alpha(q)+N(p)\to\gamma(k)+N(p')\ . \tag{12}$$

The Lorentz structure of the T matrix is[3,8,11–13]

$$T=\bar{u}(p')\sum_{i=1}^{4}A_i(s,t)M_i u(p)\ . \tag{13}$$

$A_i(s,t)$ are the invariant amplitudes; $s=(q+p)^2$ and $t=(k-q)^2$ are the Mandelstam variables. M_i are the following gauge invariance spin matrices:

$$M_1=i\gamma_5\not{\epsilon}\not{k}\ ,$$
$$M_2=2i\gamma_5(k\cdot P\epsilon\cdot q-\epsilon\cdot Pk\cdot q)\ ,$$
$$M_3=i\gamma_5(\not{\epsilon}k\cdot q-\not{k}\epsilon\cdot q)\ , \tag{14}$$
$$M_4=2i\gamma_5(\not{\epsilon}k\cdot P-\not{k}\epsilon\cdot P-m\not{\epsilon}\not{k})\ ,$$

where ϵ is the photon polarization four vector and $P\equiv\frac{1}{2}(p+p')$.

The charge structure of the amplitude is defined by

$$A_i(s,t)=A_i^{(+)}\delta_{\alpha3}+\tfrac{1}{2}[\tau_\alpha,\tau_3]A_i^{(-)}+\tau_\alpha A_i^{(0)}\ . \tag{15}$$

From the properties of the isospin matrices T_i displayed in (10) it is seen that Δ poles do not contribute to $A_i^{(0)}$.

In terms of $A_i^{(+)}$, $A_i^{(0)}$, and $A_i^{(-)}$ the π-capture amplitudes in different charged states are given by

$$A_i(\pi^0+p\to\gamma+p)=A_i^{(+)}+A_i^{(0)}\ ,$$
$$A_i(\pi^0+n\to\gamma+n)=A_i^{(+)}-A_i^{(0)}\ ,$$
$$A_i(\pi^++n\to\gamma+p)=\sqrt{2}(A_i^{(0)}-A_i^{(-)})\ , \tag{16}$$
$$A_i(\pi^-+p\to\gamma+n)=\sqrt{2}(A_i^{(0)}+A_i^{(-)})\ .$$

Using the first *four* terms in (1) we calculated the amplitudes A_i in different isospin states at the tree level (the nucleon and the pion poles and the seagull term). These amplitudes can be written in the compact form

$$\mathbf{A}^{(0,+)}(s,t)=\mathbf{S}_N\cdot\mathbf{K}^{(S,V)}+\mathbf{L}^{(S,V)}\ , \tag{17}$$

where

$$\mathbf{A}=\begin{bmatrix}A_1\\A_2\\A_3\\A_4\end{bmatrix},\quad \mathbf{K}^{(S,V)}=-\frac{ef}{m_\pi}\begin{bmatrix}m\\ \dfrac{2m}{t-m^2}\\ -\kappa^{(S,V)}\\ -\kappa^{(S,V)}\end{bmatrix},\quad \mathbf{L}^{(S,V)}=-\frac{ef}{m_\pi m}\begin{bmatrix}\kappa^{(S,V)}\\0\\0\\0\end{bmatrix}. \tag{18}$$

$\mathbf{S}_N$ is a diagonal 4×4 matrix with the following nonzero elements:

$$S_N^{11}=S_N^{22}=S_N^{44}=\frac{1}{s-m^2}+\frac{1}{u-m^2},\qquad S_N^{33}=\frac{1}{s-m^2}-\frac{1}{u-m^2}. \tag{19}$$

In (17) the superscripts 0 and + on the left-hand side go with S and V, respectively, on the right-hand side. We can also write

$$\mathbf{A}^{(-)}(s,t)=-\mathbf{Q}_N\cdot\mathbf{K}^{(V)} \tag{20}$$

where $\mathbf{Q}_N$ is a diagonal 4×4 matrix with nonzero elements,

$$Q_N^{11}=Q_N^{22}=Q_N^{44}=S_N^{33},\qquad Q_N^{33}=S_N^{11}. \tag{21}$$

The contribution of Δ-pole graphs is calculated by using the last two terms of (1). As stated earlier, Δ-pole graphs do not contribute to $A_i^{(0)}$. In matrix notation we get,

$$\mathbf{A}_\Delta^{(+)}(s,t)=2\mathbf{S}_\Delta\cdot\mathbf{K}_\Delta^{(+)}+\mathbf{L}_\Delta^{(+)}, \tag{22}$$

where $\mathbf{S}_\Delta$ is a diagonal complex matrix with nonzero entries,

$$S_\Delta^{11}=S_\Delta^{22}=S_\Delta^{44}=\frac{1}{s-m_\Delta^2+i\gamma q^3/\sqrt{s}}+\frac{1}{u-m_\Delta^2},\qquad S_\Delta^{33}=\frac{1}{s-m_\Delta^2+i\gamma q^3/\sqrt{s}}-\frac{1}{u-m_\Delta^2}. \tag{23}$$

γ is the dimensionless reduced width and q the magnitude of three momentum $\mathbf{q}$ in the πN center of mass. $\mathbf{K}_\Delta^{(+)}$ and $\mathbf{L}_\Delta^{(+)}$ are columns defined by

$$\mathbf{K}_\Delta^{(+)}=\frac{ecg^*}{3}\begin{bmatrix}\dfrac{t}{2}+\dfrac{mm_\pi^2}{6m_\Delta}\left[2+\dfrac{m}{m_\Delta}\right]+\dfrac{m}{6m_\Delta}\left[1+\dfrac{m}{m_\Delta}\right](m_\Delta^2-m^2)\\ -\frac{1}{3}(m+m_\Delta)+\dfrac{mm_\pi^2}{6m_\Delta^2}-\dfrac{(m_\Delta^2-m^2)}{6m_\Delta}\left[1-\dfrac{m}{m_\Delta}\right]\\ \frac{2}{3}(m+m_\Delta)+\dfrac{mm_\pi^2}{6m_\Delta^2}-\dfrac{(m_\Delta^2-m^2)}{6m_\Delta}\left[1-\dfrac{m}{m_\Delta}\right]\end{bmatrix}, \tag{24}$$

$$\mathbf{L}_\Delta^{(+)}=\tfrac{2}{3}ecg^*\begin{bmatrix}\dfrac{m}{3m_\Delta}+\dfrac{2m^2+m_\pi^2-t}{6m_\Delta^2}\\ 0\\ 0\\ -\dfrac{1}{3m_\Delta}\left[1-\dfrac{m}{m_\Delta}\right]\end{bmatrix}, \tag{25}$$

we also find

$$\mathbf{A}_\Delta^{(-)}=\mathbf{Q}_\Delta\cdot K_\Delta^{(-)}+\mathbf{L}_\Delta^{(-)}, \tag{26}$$

where $\mathbf{Q}_\Delta$ is a diagonal matrix with nonzero elements

$$Q_\Delta^{11}=Q_\Delta^{22}=Q_\Delta^{44}=S_\Delta^{33},\qquad Q_\Delta^{33}=S_\Delta^{11}. \tag{27}$$

The column $K_\Delta^{(-)}$ is the *same* as $K_\Delta^{(+)}$ of (24). $\mathbf{L}_\Delta^{(-)}$ is defined as

$$L_\Delta^{(-)}=\frac{ecg^*}{3}\begin{bmatrix}\dfrac{s-u}{6m_\Delta^2}\\ 0\\ -\dfrac{1}{3m_\Delta}\left[1-\dfrac{m}{m_\Delta}\right]\\ 0\end{bmatrix}. \tag{28}$$

The differential cross section and the left-right asymmetry are then calculated as follows. Define the center of

mass scattering amplitude $F(s,t)$ from the T matrix $T(s,t)$ as[8]

$$F(s,t)=\frac{m}{4\pi W}T(s,t)\ . \tag{29}$$

$F(s,t)$ is then expanded in terms of Pauli spin matrices as[8] (we use the Coulomb gauge, $\epsilon_0=0$)

$$F(s,t)=\chi_f^\dagger f(s,t)\chi_i \tag{30}$$

and

$$f(s,t)=i\boldsymbol{\sigma}\cdot\boldsymbol{\epsilon}f_1+\boldsymbol{\sigma}\cdot(\hat{\mathbf{k}}\times\boldsymbol{\epsilon})\boldsymbol{\sigma}\cdot\hat{\mathbf{q}}f_2 +i\boldsymbol{\sigma}\cdot\hat{\mathbf{k}}\boldsymbol{\epsilon}\cdot\hat{\mathbf{q}}f_3+i\boldsymbol{\sigma}\cdot\hat{\mathbf{q}}\boldsymbol{\epsilon}\cdot\hat{\mathbf{q}}f_4\ . \tag{31}$$

χ_f and χ_i are the Pauli spinors for the final and initial nucleons. $\hat{\mathbf{k}}$ and $\hat{\mathbf{q}}$ are unit vectors along the photon momentum and the pion momentum, respectively, in the center of mass frame.

Following Ref. 8 we relate f_i to A_i as follows:

$$\begin{aligned}
f_1&=\frac{(W-m)}{8\pi W}(D_1D_2)^{1/2}\left[A_1+(W-m)A_4-\frac{(t-m_\pi^2)}{2(W-m)}(A_3-A_4)\right],\\
f_2&=\frac{(W-m)}{8\pi W}\left[\frac{D_2}{D_1}\right]^{1/2}\left[A-(W+m)A_4+\frac{(t-m_\pi^2)}{2(W+m)}(A_3-A_4)\right],\\
f_3&=\frac{(W-m)}{8\pi W}(D_1D_2)^{1/2}q[-(W-m)A_2+(A_3-A_4)],\\
f_4&=\frac{(W-m)}{8\pi W}\left[\frac{D_2}{D_1}\right]^{1/2}q^2[(W+m)A_2+(A_3-A_4)],
\end{aligned} \tag{32}$$

where $D_1=m+E_1=m+(m^2+q^2)^{1/2}$ and $D_2=m+E_2=m+(m^2+k^2)^{1/2}$. With these definitions the differential cross section is given by

$$\frac{d\sigma}{d\Omega}=\frac{2k}{q}\{|f_1|^2+|f_2|^2+\tfrac{1}{2}|f_3|^2+\tfrac{1}{2}|f_4|^2+\mathrm{Re}(f_1^*f_4)-\mathrm{Re}(f_2^*f_3)+\cos\theta[2\,\mathrm{Re}(f_1^*f_2)+\mathrm{Re}(f_3^*f_4)] +\cos^2\theta[-\tfrac{1}{2}|f_3|^2-\tfrac{1}{2}|f_4|^2-\mathrm{Re}(f_1^*f_4)+\mathrm{Re}(f_2^*f_3)]-\cos^3\theta\,\mathrm{Re}(f_3^*f_4)\}\ . \tag{33}$$

The L-R asymmetry is given by

$$\begin{aligned}
A(\theta)&=\frac{\left[\frac{d\sigma}{d\Omega}\right]^{(\uparrow)}-\left[\frac{d\sigma}{d\Omega}\right]^{(\downarrow)}}{\left[\frac{d\sigma}{d\Omega}\right]^{(\uparrow)}+\left[\frac{d\sigma}{d\Omega}\right]^{(\downarrow)}}\\
&=\frac{(2k/q)}{(d\sigma/d\Omega)}\sin\theta\,\mathrm{Im}[2(f_1^*f_2)-(f_1^*f_3)-(f_2^*f_4)+(f_3^*f_4)-\cos\theta(f_1^*f_4+f_2^*f_3)-\cos^2\theta(f_3^*f_4)]\ .
\end{aligned} \tag{34}$$

The "up" direction is defined by $\hat{\mathbf{n}}=(\mathbf{q}\times\mathbf{k})/|\mathbf{q}\times\mathbf{k}|$. Time-reversal invariance implies that the L-R asymmetry parameter $A(\theta)$ in radiative π capture is equal to the recoil nucleon polarization $P(\theta)$ in pion photoproduction at the equivalent photon energy. Also, by multiplying $d\sigma/d\Omega$ of (33) by the detailed balance factor $q^2/(2k^2)$, one derives the pion photoproduction cross section at the equivalent photon energy.

III. A CALCULATION AT THE BAG LEVEL

We refer the reader to Ref. 7 for details. Here we will present only an abbreviated version of the formalism.

The effect of the bag is to give the πN-coupling constant a momentum dependence [see Eqs. (2.9) and (2.10) of Ref. 7]. We incorporate this effect by multiplying the πN-coupling constant f by a form factor

$$F(\mathbf{q}^2)=\frac{1}{F(0)}R_0(j_0^2-\tfrac{1}{3}j_1^2)\ , \tag{35}$$

where

$$\begin{aligned}
R_l(f)&\equiv N^2\int_0^R r^2dr j_l(qr)f\left[\frac{\omega}{R}r\right],\\
N^2&=\frac{\omega}{2R^3(\omega-1)j_0^2(\omega)}\ .
\end{aligned} \tag{36}$$

ω, the lowest frequency mode for massless quarks, is 2.04 and R, the bag radius is assigned two different values of 3.65 GeV^{-1} and 5.0 GeV^{-1}. The $\pi N\Delta$-coupling constant g^* $(=1.9/m_\pi)$ is also multiplied by the form factor $F(\mathbf{q}^2)$ of (35).

The reason for using the form factor only from the chiral bag model is that the chiral bag model in absence of center-of-mass corrections and the pion cloud effects predicts[2] too small a value for the pion-nucleon coupling constant. Indeed when we tried to use the chiral bag model value of pion-nucleon coupling constant to calculate the cross sections we badly underestimated them. Our procedure of using the form factor from the chiral bag model amounts to the assumption that pionic cloud effects generate[14] the experimental value of the pion-nucleon coupling constant but that the form factor would

TABLE I. Nucleon level and bag level vertices.

Nuclear level calculation	Bag level calculation
f (πN coupling constant)	$fF(\mathbf{q}^2)$
g^* ($\pi N\Delta$ coupling constant)	$g^*F(\mathbf{q}^2)$
$(1+\tau_3)$	$F_1^S(\mathbf{k}^2)+\tau_3 F_1^V(\mathbf{k}^2)$
$(\kappa^S+\tau_3\kappa^V)$	$F_2^S(\mathbf{k}^2)+\tau_3 F_2^V(\mathbf{k}^2)$
$(1+\tau_3)\tau_\alpha$	$\tau_\alpha F_1^S(\mathbf{k}^2)+\delta_{3\alpha}F_1^V(\mathbf{k}^2)$ $-\frac{1}{2}[\tau_\alpha,\tau_3]F_1^V(\mathbf{k}^2)$

be given by the chiral bag model.

In Table I we have summarized the replacements one has to make in going from a nucleon level calculation to a bag level calculation. The net effect of the replacements shown in Table I is that the columns $\mathbf{K}^{(S,V)}$ and $\mathbf{L}^{(S,V)}$ of (18) are now modified to read

$$\mathbf{K}^{(S,V)}\xrightarrow{\text{bag}}-\frac{efF(q^2)}{m_\pi}\begin{bmatrix} mF_1^{(S,V)} \\ \dfrac{2m}{t-m_\pi^2}F_1^{(S,V)} \\ -F_2^{(S,V)} \\ -F_2^{(S,V)}\end{bmatrix}, \tag{37}$$

$$\mathbf{L}^{(S,V)}\xrightarrow{\text{bag}}-\frac{efF(\mathbf{q}^2)}{m_\pi m}\begin{bmatrix} F_2^{(S,V)} \\ 0 \\ 0 \\ 0\end{bmatrix}. \tag{38}$$

The relation between $F_{1,2}^{(S,V)}(\mathbf{k}^2)$ and the electric and magnetic form factors $G_E(\mathbf{k}^2)$ and $G_M(\mathbf{k}^2)$ is given in Eqs. (2.22) to (2.26) of Ref. 7. Here we transcribe these equations in a slightly different form

$$\begin{aligned}
F_1^S(\mathbf{k}^2)&=\left[1+\frac{\mathbf{k}^2}{4m^2}\right]^{-1}\left[G_E^0(\mathbf{k}^2)+\frac{\mathbf{k}^2}{12m^2}G_M^0(\mathbf{k}^2)\right],\\
F_1^V(\mathbf{k}^2)&=\left[1+\frac{\mathbf{k}^2}{4m^2}\right]^{-1}\left[G_E^0(\mathbf{k}^2)+\frac{5}{12}\frac{\mathbf{k}^2}{m^2}G_M^0(\mathbf{k}^2)\right],\\
F_2^S(\mathbf{k}^2)&=\left[1+\frac{\mathbf{k}^2}{4m^2}\right]^{-1}\left[\tfrac{1}{3}G_M^0(\mathbf{k}^2)-G_E^0(\mathbf{k}^2)\right],\\
F_2^V(\mathbf{k}^2)&=\left[1+\frac{\mathbf{k}^2}{4m^2}\right]^{-1}\left[\tfrac{5}{3}G_M^0(\mathbf{k}^2)-G_E^0(\mathbf{k}^2)\right],
\end{aligned} \tag{39}$$

where $G_E^0(\mathbf{k}^2)$ and $G_M^0(\mathbf{k}^2)$ are defined in Eqs. (2.24)–(2.29) of Ref. 7. We reproduce the final forms,

$$\begin{aligned}
G_E^0(\mathbf{k}^2)&=R_0(j_0^2+j_1^2),\\
G_M^0(\mathbf{k}^2)&=\frac{2m}{k}R_1(2j_0j_1).
\end{aligned} \tag{40}$$

Finally the constant C is replaced by [see (2.36) of Ref. 7]

$$C\xrightarrow{\text{bag}}\frac{2\sqrt{2}}{3m+m_\Delta}G_M^0(\mathbf{k}^2). \tag{41}$$

It is well known[2,7,15] that the chiral bag model prediction of $G_M^0(0)$, which is directly related[7,15] to the proton magnetic moment μ_p, is too low. Indeed when we tried to use the value of C in (41) with $G_M^0(\mathbf{k}^2)$ given[7,15] by the chiral bag model the calculated cross sections for reactions involving neutral pions, $\pi^0 p\rightleftarrows\gamma p$ and $\pi^0 n\rightleftarrows\gamma n$, turned out to be too low for any reasonable bag radius. This is not surprising since the value of C used in the nucleon level calculation is $0.32/m_\pi$ [see Eq. (6)] while with $R=5$ GeV^{-1}, (41) gives $C=0.2/m_\pi$ at $\mathbf{k}^2=0$. A smaller bag radius makes matters worse. Again we took the attitude that pionic cloud effects (and center-of-mass corrections) would raise the predicted value of $G_M^0(0)$. We hence normalized $G_M^0(0)$ to give the proton magnetic moment correctly. This assumption amounts to using the chiral bag model only for the momentum dependence of $G_M^0(\mathbf{k}^2)$. In doing the bag calculation there is a technical problem of enforcing gauge invariance due to the appearance of form factors. This is done "by hand."

IV. RESULTS AND DISCUSSION

We have calculated the differential cross sections and L-R asymmetry for radiative pion capture in all charged combinations. Since the pion capture data is rather sparse we have also calculated the pion photoproduction differential cross section through detailed balance. Time-reversal invariance also makes the L-R asymmetry in radiative pion capture equal to the recoil nucleon po-

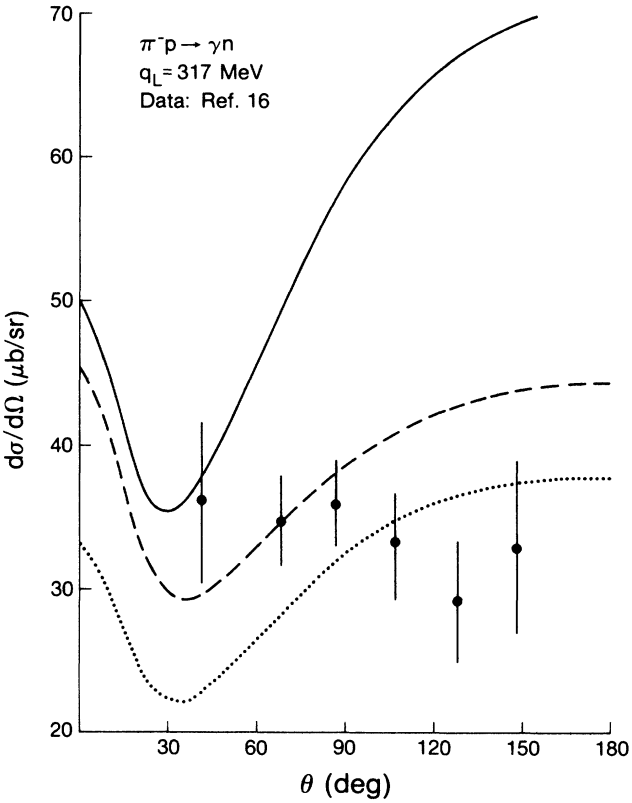

FIG. 1. $d\sigma/d\Omega$ and $A(\theta)$ for $\pi^- p\rightarrow\gamma n$ at $q_L=317$ MeV. Solid curve, nucleon level calculation; dashed curve, bag model with $R=3.65$ GeV^{-1}; dotted curve, bag model with $R=5.0$ GeV^{-1}. Data: Ref. 16.

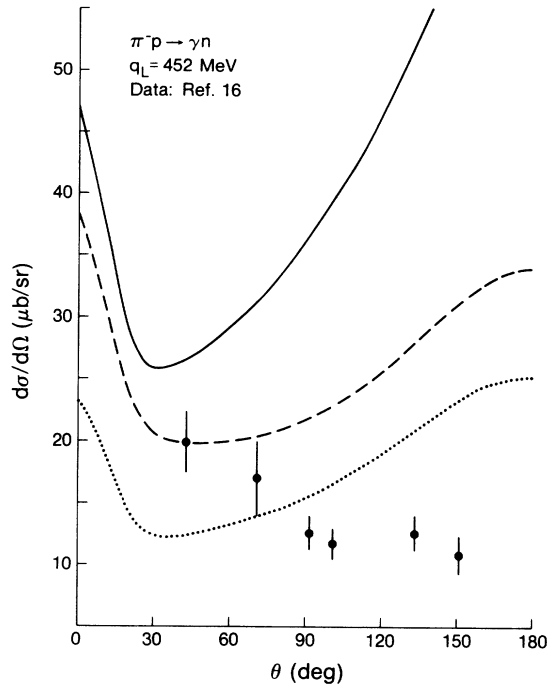

FIG. 2. $d\sigma/d\Omega$ and $A(\theta)$ for $\pi^- p \to \gamma n$ at $q_L = 452$ MeV. Theoretical curves identified as in Fig. 1. Data: Ref. 16.

larization in pion photoproduction at an appropriate photon energy.

Differential cross sections for the radiative pion capture process $\pi^- p \to \gamma n$ have been measured at pion laboratory momenta $q_L = 317$, 452, and 491 MeV by Berardo *et al.*[16] In Figs. 1–3 we have shown our calculated $d\sigma/d\Omega$ vs θ (in the center of mass) together with the data of Ref. 16. From the $d\sigma/d\Omega$ plots it is clear that

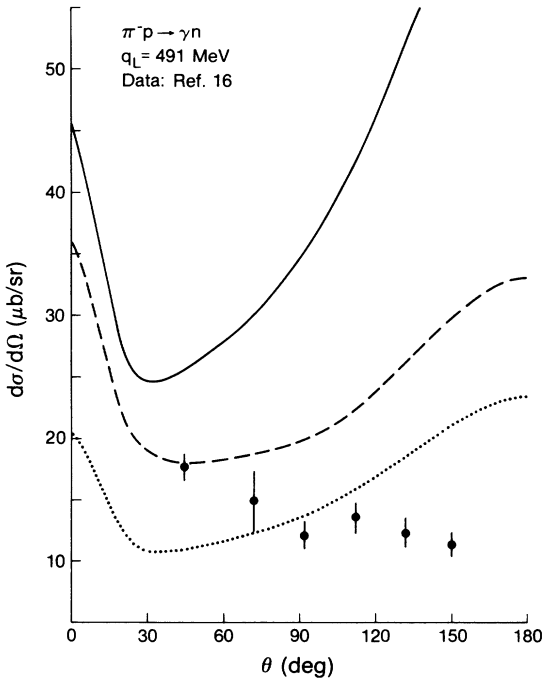

FIG. 3. $d\sigma/d\Omega$ and $A(\theta)$ for $\pi^- p \to \gamma n$ at $q_L = 491$ MeV. Theoretical curves identified as in Fig. 1. Data: Ref. 16.

the nucleon level calculation overestimates the cross section both in the forward and the backward directions. The backward peaking in $\pi^- p \to \gamma n$ is associated with the u-channel nucleon pole. It is worth noting that the u-channel nucleon pole contribution is considerably suppressed in $\pi^+ n \rightleftarrows \gamma p$ reactions since the particle exchanged in the u channel is a neutron. The bag model calculation tends to suppress the backward peak due to the electromagnetic form factor effects. The cross sections calculated in the bag model are lower than those in the nucleon level calculation. Although this is a distinct improvement, the agreement with experiments is far from good. Data in forward directions ($\theta < 30°$) would help. The data in the interval $40° < \theta < 150°$ show no tendency to rise in the backward direction. Moreover, there is no evidence of a dip around 30° which the theoretical calculations show. If the rise in the differential cross section in the backward direction could be suppressed, the dip around 30° would also be eliminated. Inclusion of other nucleon resonances, such as $N(1440)$, in the u channel could help suppress the backward rise in $d\sigma/d\Omega$.

In Fig. 4 we have plotted the L-R asymmetry at four different pion laboratory momenta: $q_L = 427$, 471, 547, and 625 MeV. Data exist[17] at these momenta. We have not shown the data in our plots since Ref. 17 does not provide a tabulation of the measured asymmetry. However, a comparison of our calculated L-R asymmetry with the plots of Ref. 17 shows that our calculated asymmetries fare quite well at $q_L = 427$ MeV but progressively worse at higher momenta. The predicted L-R asym-

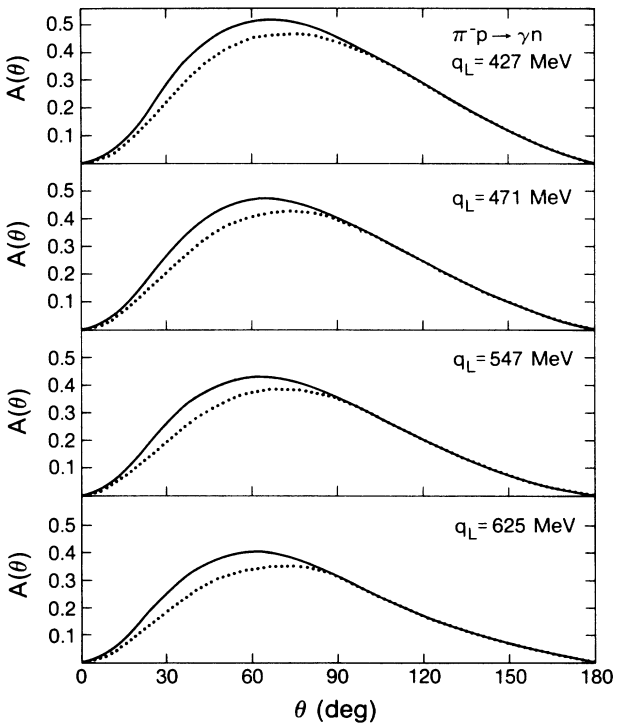

FIG. 4. $A(\theta)$ for $\pi^- p \to \gamma n$ at $q_L = 472$, 471, 547, and 625 MeV. Theoretical curves identified as in Fig. 1. Bag predictions use $R = 5.0$ GeV^{-1} ($R = 3.65$ GeV^{-1} results are almost identical). See Ref. 17 for data.

metry shows very little energy dependence. The reason for this is that the imaginary part of the amplitude is generated in our model calculation by the width of the Δ propagator in the direct channel. The real and the imaginary parts of the calculated amplitudes are fairly smooth functions of energy. The energy dependence of data[17] at higher energies than $q_L = 427$ MeV is presumably due to higher nucleon resonances, such as $N(1440)$, in the direct channel, contributing to the imaginary part of the amplitude at larger incident momenta.

In Fig. 5 we have plotted $d\sigma/d\Omega$ for $\gamma n \to \pi^- p$ obtained by using detailed balance at laboratory photon momenta $k_L = 340$, 430, and 530 MeV. We notice that the bag model calculation with either radius, $R = 3.65$ GeV^{-1} or 5.0 GeV^{-1}, fares better than the nucleon level calculation. This is to be expected from our discussion above of the results for the inverse reaction $\pi^- p \to \gamma n$ at similar energies. The backward peaking of the nucleon level calculation of $d\sigma/d\Omega$ is due to the nucleon (proton) pole in the u channel. The bag model calculation tends to suppress the backward rise, although not enough to fill in the dip at $\theta \approx 30°$–$40°$. The calculation with $R = 5.0$ GeV^{-1} does marginally better than the one with $R = 3.65$ GeV^{-1}.

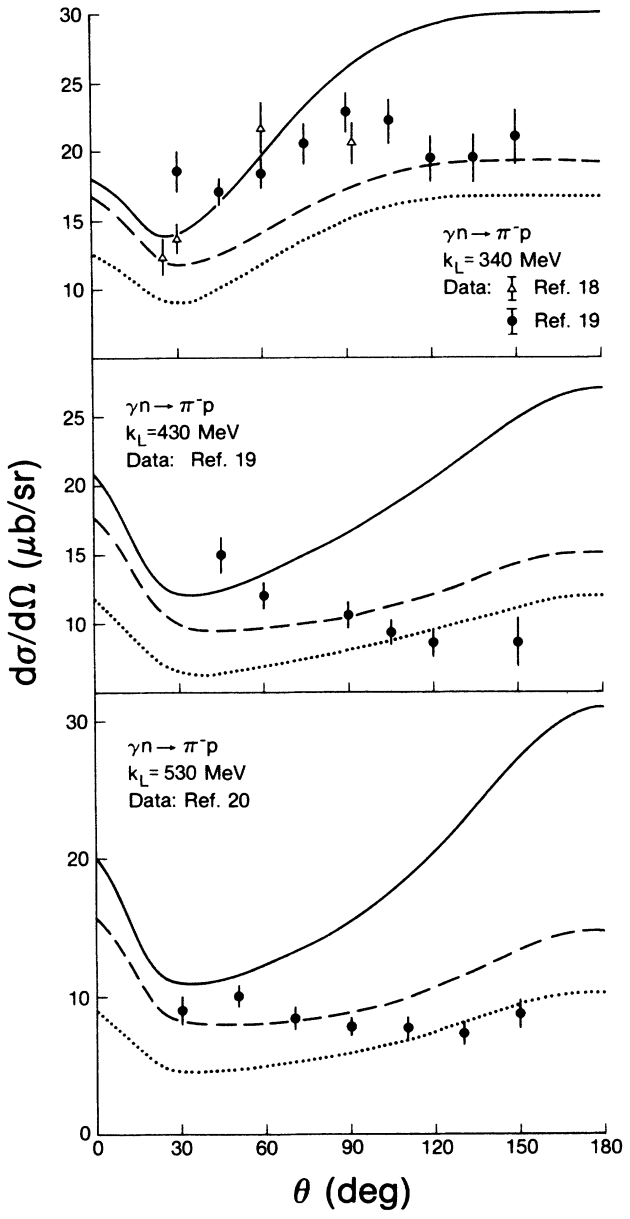

FIG. 5. $d\sigma/d\Omega$ vs θ for $\gamma n \to \pi^- p$ extracted through detailed balance at $k_L = 340$ MeV (data: Refs. 18 and 19; Ref. 18 is a pion capture experiment); $k = 430$ MeV (data: Ref. 19) and $k_L = 530$ MeV (data: Ref. 20). Dashed curve, $R = 3.65$ GeV^{-1}; dotted curve, $R = 5$ GeV^{-1}.

In Fig. 6 we have plotted our calculated $d\sigma/d\Omega$ for $\gamma p \to \pi^+ n$, using detailed balance, at $k_L = 340$, 430, and 530 MeV. The nucleon level calculation does quite well at $k_L = 340$ MeV. The bag model, particularly the one with $R = 5.0$ GeV^{-1}, does fairly well at higher photon energies. The trend of falling cross-sections at the backward angles at $k_L = 430$ and 530 MeV is not reproduced by our calculations.

In Fig. 7 we have plotted our calculated $d\sigma/d\Omega$ for $\gamma p \to \pi^0 p$ at $k_L = 340$, 430, and 530 MeV. Here the bag

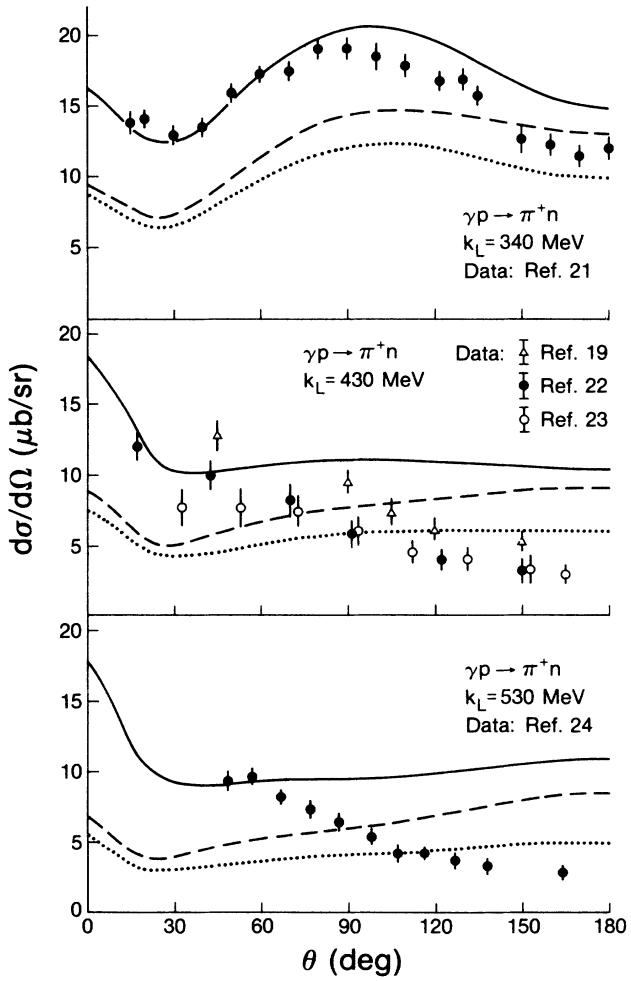

FIG. 6. $d\sigma/d\Omega$ vs θ for $\gamma p \to \pi^+ n$ extracted through detailed balance at $k_L = 340$ MeV (data: Ref. 21), $k_L = 430$ MeV (data: Refs. 19, 22, and 23) and $k_L = 530$ MeV (data: Ref. 24). Dashed curve, $R = 3.65$ GeV^{-1}; dotted curve, $R = 5$ GeV^{-1}.

model estimates are too low by almost a factor of 2. The nucleon level calculation appears to do better than the bag model calculations particularly at higher photon energies.

In Fig. 8 we have plotted the recoil nucleon polarization in $\gamma p \to \pi^+ n$ at laboratory photon energies $k_L = 340$ MeV and 530 MeV and in $\gamma p \to \pi^0 p$ at $k_L = 340$ MeV. These polarizations are the same as the L-R asymmetry in radiative pion capture at laboratory pion momenta $q_L = 300$ MeV (corresponding to $k_L = 340$ MeV) and $q_L = 500$ MeV). The polarization at $k_L = 340$ MeV appears to be well reproduced by both the nucleon level calculation and the bag model calculation with bag radius $R = 5.0$ GeV^{-1}. At $k_L = 530$ MeV neither calculation reproduces data in the forward angles.

In summary, the chiral bag model calculations appear to reproduce $d\sigma/d\Omega$ for $\pi^- p \to \gamma n$ at $q_L = 317$ MeV with the nucleon and Δ-resonance contributions. Agreement with data declines at $q_L = 452$ and 491 MeV. Our model calculation for L-R asymmetry shows the same trend. We anticipate that at higher incident pion momenta the contribution from higher resonances such as $N(1440)$ would be significant and complex. The L-R asymmetry should be sensitive to $N(1440)$ contribution at higher energies.

Our model bag calculation of $d\sigma/d\Omega$ for $\gamma n \to \pi^- p$ appears to do well in the region $k_L = 300$–500 MeV. For $\gamma p \to \pi^+ n$ the agreement with data declines at energies $k_L = 450$–550 MeV. For $\gamma p \to \pi^0 p$ our calculations, including those at the nucleon level, underestimate the cross sections at all energies, although the angular dependence has the correct shape. A reliable calculation at higher energies ($q_L \gtrsim 500$ MeV) must include the effect of higher resonances. This is particularly true of the polarization and L-R asymmetry.

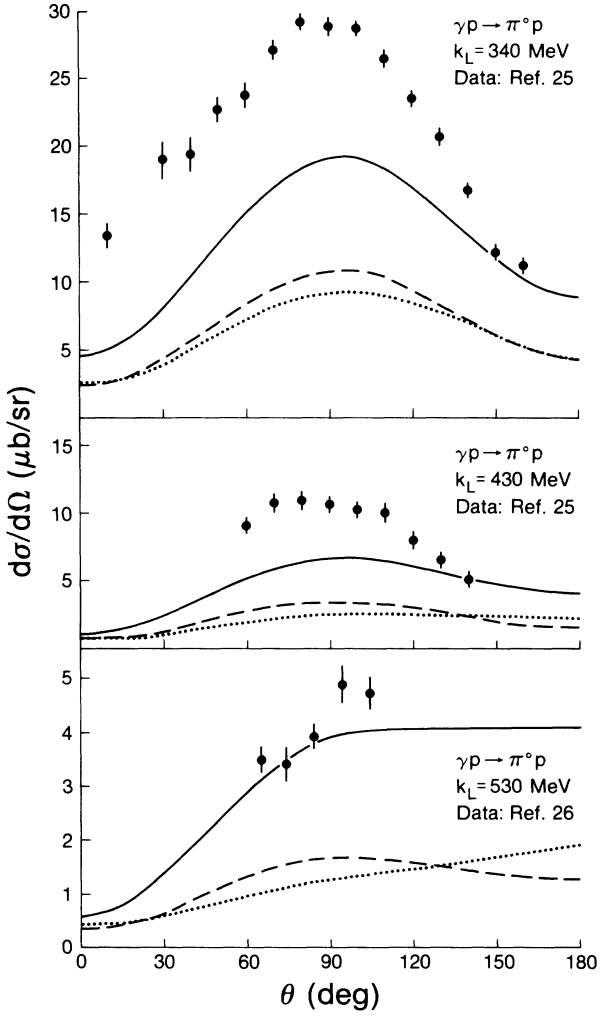

FIG. 7. $d\sigma/d\Omega$ vs θ for $\gamma p \to \pi^0 p$ extracted through detailed balance at $k_L = 340$ MeV (data: Ref. 25), $k_L = 430$ MeV (data: Ref. 25) and $k_L = 530$ MeV (data: Ref. 26). Dashed curve, $R = 3.65$ GeV^{-1}; dotted curve, $R = 5.0$ GeV^{-1}.

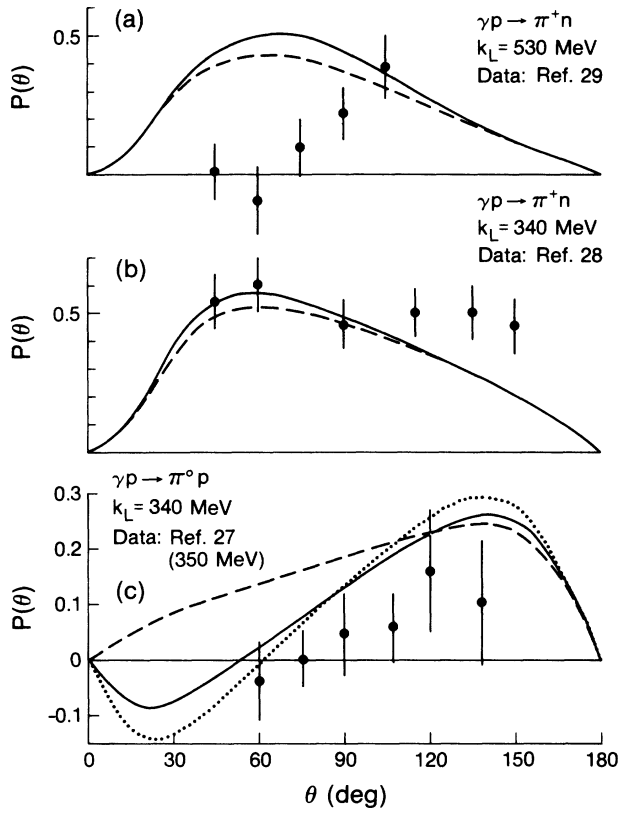

FIG. 8. $P(\theta)$ vs θ. (a) $\gamma p \to \pi^+ n$ at $k_L = 530$ MeV (data: Ref. 29). (b) $\gamma p \to \pi^+ n$ at $k_L = 340$ MeV (data: Ref. 28). $P(\theta)$ for $R = 3.65$ GeV^{-1} and $R = 5.0$ GeV^{-1} are almost indistinguishable. (c) $\gamma p \to \pi^0 p$ at $k_L = 340$ MeV (data: Ref. 27). Dashed curve, $R = 3.65$ GeV^{-1}; dotted curve, $R = 5.0$ GeV^{-1}. $P(\theta)$ in photoproduction equals L-R asymmetry in pion capture at the appropriate energy.

This research was partly supported by a grant to A. N. K. from the Natural Sciences and Engineering Research Council of Canada.

[1]A. Chodos, R. L. Jaffe, K. Johnson, C. B. Thorn, and V. F. Weisskopf, Phys. Rev. D **9**, 3491 (1974); K. Johnson, Acta Phys. Pol. B **6**, 865 (1975); T. A. DeGrand, R. L. Jaffe, K. Johnson, and J. Kiskis, Phys. Rev. D **12**, 2060 (1975).
[2]S. Théberge, A. W. Thomas, and G. A. Miller, Phys. Rev. D **22**, 2838 (1980); **23**, 2106(E) (1981); Can. J. Phys. **60**, 59 (1982).
[3]G. F. Chew, M. L. Goldberger, F. E. Low, and Y. Nambu, Phys. Rev. **106**, 1345 (1957).
[4]S. Weinberg, Phys. Rev. Lett. **17**, 616 (1966).
[5]A. W. Thomas, J. Phys. G **7**, L283 (1981).
[6]G. Kälberman and J. M. Eisenberg, Phys. Rev. D **28**, 66 (1983); **28**, 71 (1983).
[7]M. Araki and A. N. Kamal, Phys. Rev. D **29**, 1345 (1984).
[8]M. G. Olsson and E. T. Osypowski, Nucl. Phys. **B87**, 399 (1975).
[9]J. D. Bjorken and S. D. Drell, *Relativistic Quantum Fields* (McGraw-Hill, New York, 1965).
[10]H. W. Huang, Phys. Rev. **174**, 1799 (1968).
[11]N. Dombey and B. J. Read, Nucl. Phys. **B60**, 65 (1973).
[12]F. A. Berends, A. Donnachie, and D. L. Weaver, Nucl. Phys. **B4**, 1 (1967); **B4**, 54 (1967); **B4**, 103 (1967).
[13]J. M. Laget, Phys. Rep. **69**, 1 (1981).
[14]B. C. Pearce and I. R. Afnan, Phys. Rev. C **34**, 991 (1986).
[15]M. Araki and I. R. Afnan, Phys. Rev. C **36**, 250 (1987).
[16]P. A. Berardo *et al.*, Phys. Rev. D **9**, 621 (1974).
[17]G. J. Kim *et al.*, Phys. Rev. Lett. **56**, 1779 (1986).
[18]M. T. Tran *et al.*, Nucl. Phys. **A324**, 301 (1979).
[19]T. Fujii *et al.*, Nucl. Phys. **B120**, 395 (1977).
[20]P. Benz *et al.*, Nucl. Phys. **B65**, 158 (1973).
[21]G. Fischer *et al.*, Z. Phys. **253**, 38 (1972).
[22]R. L. Walker *et al.*, Phys. Rev. **99**, 210 (1955).
[23]A. V. Tollestrup, J. C. Keck, and R. M. Worlock, Phys. Rev. **99**, 220 (1955).
[24]H. A. Thiessen, Phys. Rev. **155**, 1488 (1967).
[25]H. Genzel *et al.*, Z. Phys. **268**, 43 (1974).
[26]M. Yoshioka *et al.*, Nucl. Phys. **B168**, 222 (1980).
[27]A. A. Belyaev *et al.*, Nucl. Phys. **B213**, 201 (1982).
[28]V. A. Get'man *et al.*, JETP Lett. **30**, 82 (1979).
[29]P. J. Bussey *et al.*, Nucl. Phys. **B154**, 205 (1979).